Turbulent dynamos: Experiments, nonlinear saturation of the magnetic field and field reversals

C. Gissinger & C. Guervilly

November 17, 2008

1 Introduction

Magnetic fields are present at almost all scales in the universe, from the Earth (roughly 0.5 G) to the Galaxy (10^{-6} G). It is commonly believed that these magnetic fields are generated by dynamo action *i.e.* by the turbulent flow of an electrically conducting fluid [12]. Despite this space and time disorganized flow, the magnetic field shows in general a coherent part at the largest scales. The question arising from this observation is the role of the mean flow: Cowling first proposed that the coherent magnetic field could be due to coherent large scale velocity field and this problem is still an open question.

2 MHD equations and dimensionless parameters

The equations describing the evolution of a magnetohydrodynamical system are the equation of Navier-Stokes coupled to the induction equation:

$$\frac{\partial \mathbf{v}}{\partial t} + (\mathbf{v}\cdot\nabla)\mathbf{v} = -\nabla\pi + \nu\Delta\mathbf{v} + \mathbf{f} + \frac{\mathbf{1}}{\mu\rho}(\mathbf{B}\cdot\nabla)\mathbf{B}\ , \tag{1}$$

$$\frac{\partial \mathbf{B}}{\partial t} = \nabla\times(\mathbf{v}\times\mathbf{B}) + \eta\,\Delta\mathbf{B}\ . \tag{2}$$

where $\mathbf{v}$ is the solenoidal velocity field, $\mathbf{B}$ the solenoidal magnetic field, $\nabla\pi$ the pressure gradient in the fluid, ν the kinematic viscosity, $\mathbf{f}$ a forcing term, μ the magnetic permeability, ρ the fluid density and η the magnetic permeability.

Dealing with the geodynamo, the minimal set of parameters for the outer core are :

- ρ : density of the fluid
- μ : magnetic permeability

- ν : kinematic diffusivity
- σ: conductivity
- R : radius of the outer core
- V : typical velocity
- Ω : rotation rate

The problem involves 7 independent parameters and 4 fundamental units (length L, time T, mass M and electic current A). Therefore there are 3 dimensionless parameters: the magnetic Reynolds number $Rm = \mu_0 \sigma V R$, the Reynolds number $Re = VR/\nu$ and the Rossby number $Ro = V/(R\Omega)$. One can also define the magnetic Prandtl number $Pm = \nu\mu_0\sigma = Rm/Re$.

3 Numerical simulations, experiments and the universe

In 1995, the first direct numerical simulation of dynamo was obtained by Glatzmaier and Roberts [11]. The magnetic structure observed was very similar to the Earth's one but dimensionless parameters are up to ten orders of magnitude away from realistic values. For instance, Pm is of order 1 in these simulations whereas it is 10^{-5} in the Earth.

On the figure 1, we can observe that the experiments are closer to the natural objects in term of Pm than the numerical simulations. This situation is a strong motivation to carry out dynamo experiments. In such experiments, liquid sodium is used instead of liquid iron due to the higher electric conductivity. However taking into account rotation, the situation is more dramatical for experiments since there is more than ten order of magnitude for Rossby number between the Earth and experiments. Dynamo action can only occur for sufficient Rm, typically greater than 10. Since the Prandtl number is 10^{-5} in experiments, this yields very large Reynolds number $Re > 10^6$ and consequently very turbulent flow. The power needed to drive the flow is typically $P \sim \rho V^3 R^2 f(Re)$. Because of the low value of the viscosity, Re will be dropped in first approximation in the previous relation. This leads to

$$Rm \sim \mu_0 \sigma \left(\frac{PR}{\rho} \right)^{1/3} \tag{3}$$

Using liquid sodium, 100 kW are required to reach $Rm = 50$ with $R = 1m$. Moreover, to increase Rm by a factor 10, P should be increase by a factor 1000.

The first experimental dynamos were independently observed in 2001 in Riga [8], Latvia and Karlsruhe [19], Germany. Both experiments are based on analytical flows known to produce dynamo action for relatively low Rm.
The Riga experiment is based on the Ponomarenko flow with a well known dynamo threshold. It consists of a cylindrical pipe divided into three cylindrical shells. The external one is filled with liquid sodium at rest. The internal vessel contains an downward helical flow and the fluid recirculates upward in the intermediate shell (figure 2). The experimental

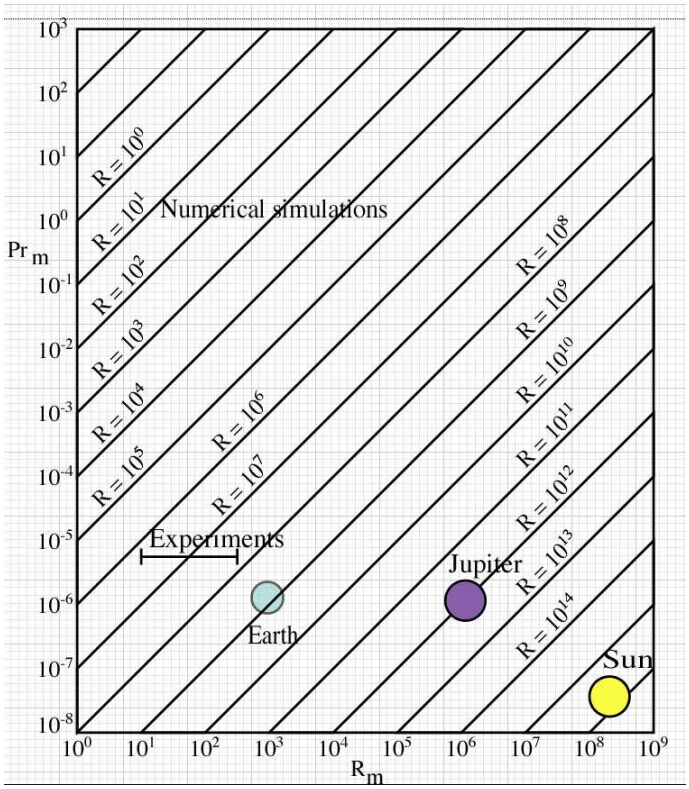

Figure 1: Parameter range for numerical simulations, experiments and natural systems.

threshold was found to be in good agreement with theoretical predictions. Moreover the Hopf bifurcation observed matched theory. The agreement between experiment and laminar kinematic dynamo theory is remarkable. However, using the non-linear theory the value of the satured magnetic field is underestimated by a factor 10^6.
The Karlsruhe experiment is based on the G.O. Roberts flow consisting in an array of whirling flow composed with azimuthal and axial flows (figure 2). The kinematic helicity defined by $(\nabla \times \mathbf{u}) \cdot \mathbf{u}$ is the same in all the pipes. The large scale magnetic field observed in this experiment involves an $\alpha -$ effect due to small scale flow. The threshold decreases when the large length scale increases but not if one decreases the small length scale.
In both experiments, the magnetic field is generated as if the mean flow were acting alone. This is probably due to the fact that the level of turbulence in these experiments is limited by the constraint of the pipes containing the flow.

The flow is very constrainted in these two experiments and does not allow to study the effect of the turbulence on the dynamo action. In the situation of a bifurcation from a strongly turbulent flow, two questions arise:

- What is the effect of the turbulence on the dynamo threshold?
- What is the value of the saturated magnetic field above the dynamo threshold?

In order to study a turbulent flow, it can be useful to define the Reynolds decomposition

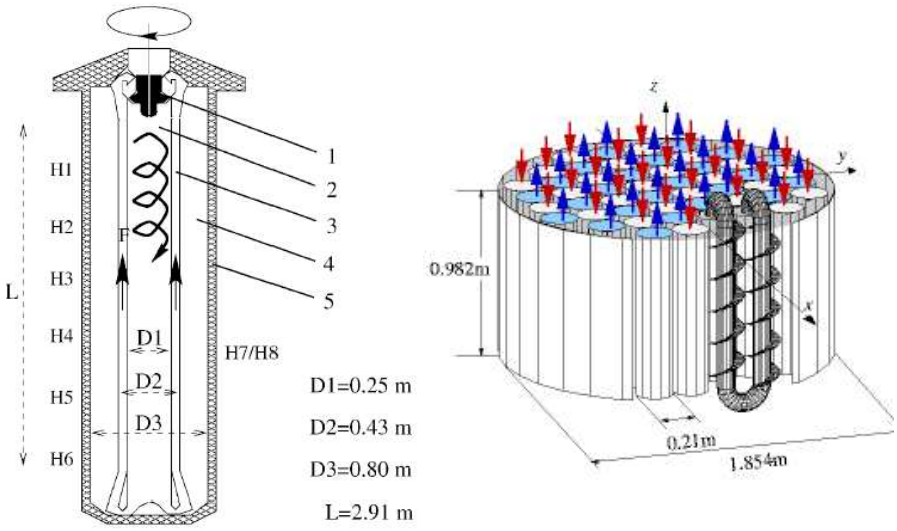

Figure 2: First experimental dynamos in constrained flows. Left: Riga experiment; Right: Karlsruhe experiment.

for the velocity field:

$$\mathbf{V}(\mathbf{r},t) = \langle \mathbf{V} \rangle(\mathbf{r}) + \tilde{\mathbf{v}}(\mathbf{r},t) \tag{4}$$

where $\langle \mathbf{V} \rangle$ represents the mean flow and $\tilde{\mathbf{v}}$ stands for the turbulent fluctuations. Then, the induction equation becomes

$$\frac{\partial \mathbf{B}}{\partial t} = \nabla \times (\langle \mathbf{V} \rangle(\mathbf{r}) \times \mathbf{B}) + \nabla \times (\tilde{\mathbf{v}}(\mathbf{r}) \times \mathbf{B}) + \eta \Delta \mathbf{B} \ . \tag{5}$$

We see that the mean flow like the turbulent fluctuations can act as a source term for the magnetic field. There is two different approach for such problem: one can try to avoid large scale fluctuations using forced flow, like in Riga or Karlsruhe experiment. Another approach is to study the effect of velocity fluctuations on the dynamo instability which is the purpose of the VKS experiment.

4 The VKS experiment

4.1 Experimental set-up

The VKS (Von Karman Sodium) dynamo [13] is based on the so called Von Karman flow (figure 3). It consists of two toroidal cells in contrarotation driven by two impellers with 8 blades. Between two successive blades, the centrifugal flow is strongly expelled, creating a pumping of the flow near the axis. Both poloidal recirculation and azimuthal flow create a strongly turbulent velocity field with an important shear layer in the midplane due to the differential rotation. This flow is also known to produce a strong helical flow. The VKS flow is carried out in a cylindrical vessel, a geometry which, because of the fast rotation of

the Earth, appears to be not so far from a geodynamo situation. In this experiment the seed field is the magnetic field of the Earth.

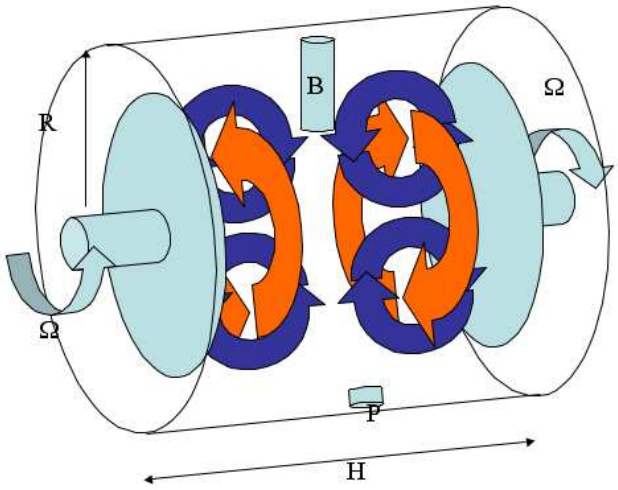

Figure 3: Sketch of the VKS flow.

There are other experimental attempts to observe self generation of magnetic field in a non-forced flow. The Madison experiment [7], in the University of Wisconsin, is based on Dudley & James flow and has been built to create a magnetic field due to this mean flow. Trials to observe dynamo in spherical couette flow, *i.e.* flow between two spherical shells in differential rotation are also made: the DTS (Derviche-Tourneur Sodium) experiment in Grenoble [14] and the Maryland experiment [18].

In the VKS experiment, 150-liters of liquid sodium are driven by the impellers with a power input of 300 kW. The temperature is monitored and 3 types of measurement are made: power, pressure and magnetic field. The last modification leading to the observation of a self-sustained magnetic field is the use of Iron discs with a strong magnetic permeability. This modification is known to reduce the threshold of the dynamo by changing the boundary conditions for the magnetic field [10]. The coercive field of the discs is close to 1 Gauss which is small compared to the magnitude of the magnetic field observed (100 G).

4.2 Results and interpretation

In exact contrarotation, first the generated magnetic field shows an exponential growth during the kinematic stage and then saturates at a strongly fluctuating state. The magnetic field is stationary and strongly axisymmetric. Generally the azimuthal part dominates the other components except near the axis, where the field is roughly an axial dipole. Figure 5 shows a typical evolution of the magnetic field of VKS.

The control parameter of the dynamo is the magnetic Reynolds number Rm. In the experiment, Rm can be varied by increasing the rotation rate of the propellers or by varying

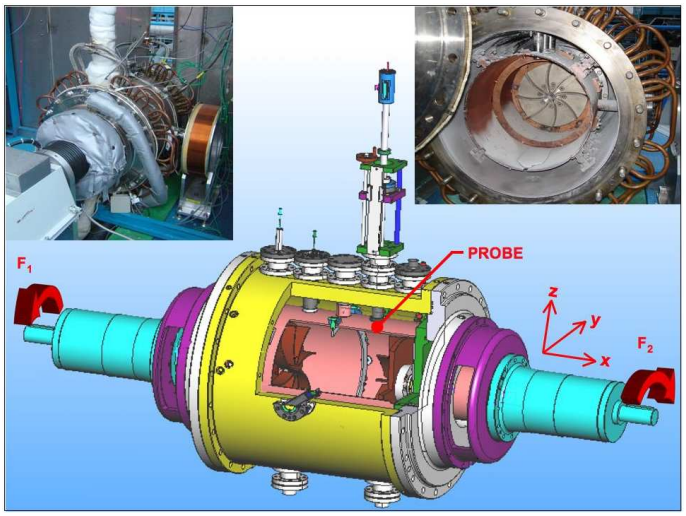

Figure 4: Sketch of the VKS experiment.

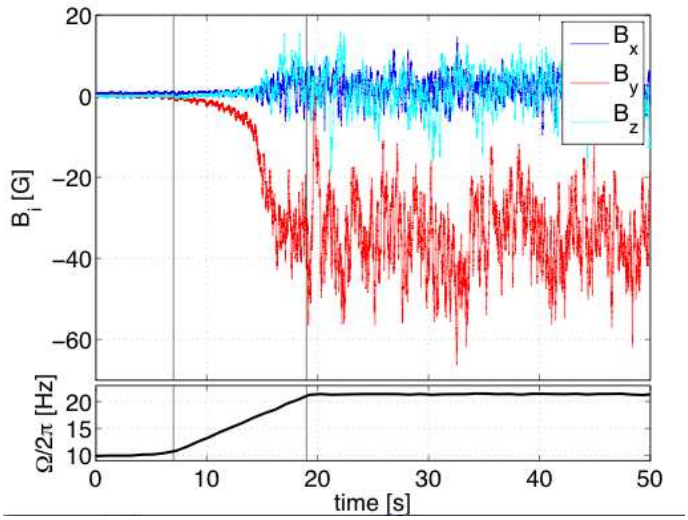

Figure 5: Time evolution of the magnetic field in the VKS experiment when the rotation rate of the discs is increased.

the temperature (and so the conductivity of sodium). The dynamo instability is a supercritical bifurcation with a threshold around $Rm_c = 30$. The saturated value of the magnetic field is in relatively good agreement with theoretical predictions (see lecture 2).

The generation of this magnetic field is understood as an $\alpha - \omega$ process [15]: due to the differential rotation between the two discs, the poloidal field is converted into a toroidal field by the so called ω-effect. In addition, the helicity of the flow will produce poloidal field from toroidal one: this α-effect is created by the flow near each disk. Between two successive blades of a disc, a strong centrifugal flow with helicity is created (figure 6). Thus, the VKS

dynamo is driven by the turbulent non-axisymmetric part of the flow. Indeed, numerical simulations based on the large scale mean flow alone always predicts an equatorial dipole breaking axisymmetry, in agreement with Cowling's theorem.

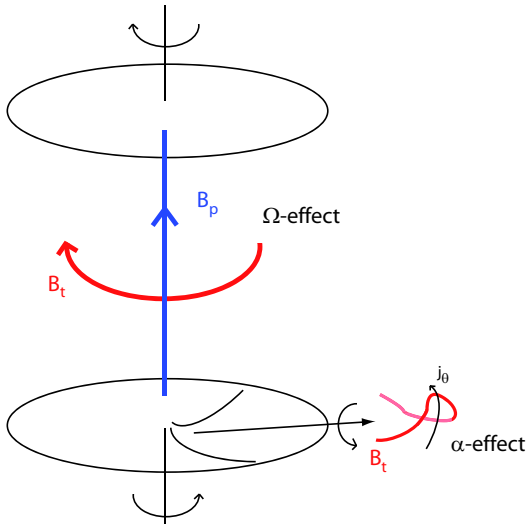

Figure 6: α and ω mechanisms in the VKS experiment.

Cowling's theorem states that an axisymmetric velocity field can not maintain an axisymmetric magnetic field. Because of the axisymmetrical nature of the forcing and the mean flow in the VKS experiment, one can be surprised by the observation of a strongly axisymmetric magnetic field. In fact, turbulent fluctuations have often been invoked to break the restriction imposed by Cowling's theorem. More surprising, even without such velocity fluctuations, it is possible to bypass the constraint of Cowling's theorem by a secondary bifurcation (figure 7). Indeed, the axisymmetric mean flow always generates a magnetic field breaking the axisymmetry, for instance an equatorial dipole in the case of the VKS experiment. The feedback of the Lorentz force immediatly creates non-axisymmetric components in the velocity field, offering a way for the system to generate an axisymmetric magnetic field. This self-killing nature of the theorem can yield complex behavior like competition between equatorial and axial dipoles [9].

In the VKS experiment, the parameter space can be explored by imposing different rotation rates for each disk (non-exact counter-rotation). The figure 8 shows the different dynamics in the parameter space when the frequency of the propellers is modified. Three kinds of dynamics are observed: stationary, oscillatory and intermittent dynamos. Chaotic field reversals are also observed [2].

For example, decreasing the rotation rate of one propeller from 11 to 10 Hz and keeping the other one constant(28 Hz) yields a transition between a stationary regime to an oscillation. One can also notice subcritical bifurcation between oscillations and stationary field in the presence of bistability (figure 9). However, no transition occurs between the two

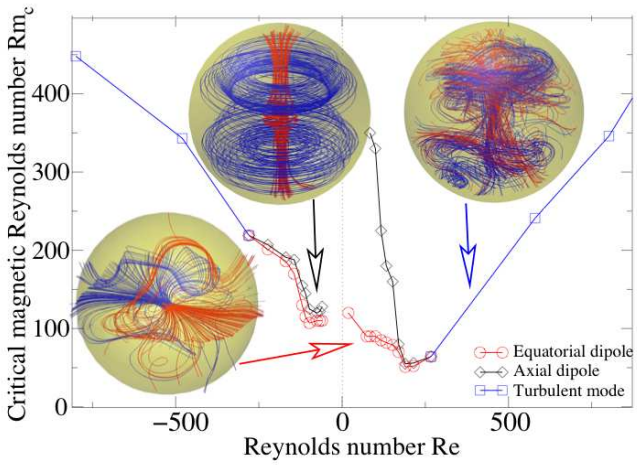

Figure 7: Numerical simulation showing how axial dipole can be generated using an axisymmetric forcing.

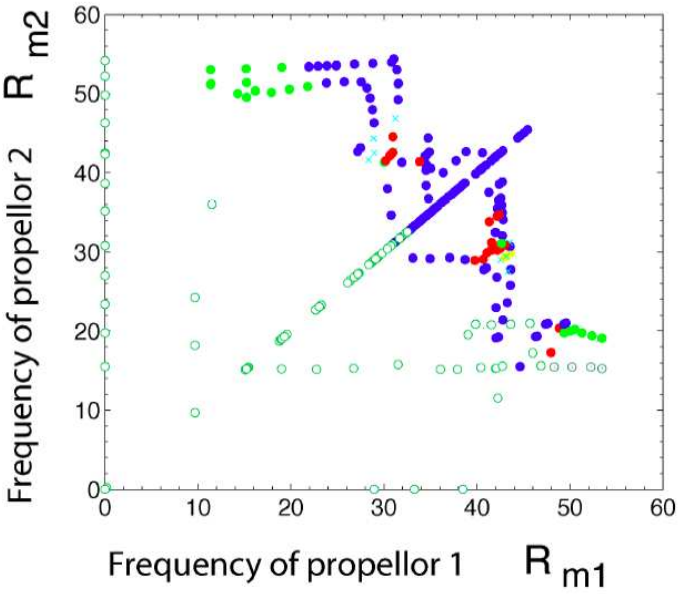

Figure 8: Different kinds of dynamics in the parameter space: open: no dynamo; closed dark: stationary dynamo; closed light: reversals and oscillatory dynamos

metastable regimes generated by the turbulent fluctuations on observable time scales.

The exploration of the parameter space shows that in non-exact counter-rotation, the observed relaxation oscillations bifurcate from fixed points located on the limit cycle as in the case of an excitable system. A very simple example of excitable system is a pendulum submitted to a constant torque. Indeed, when one apply a constant torque to a pendulum, the classical fixed points 0 (stable) and π (unstable) are respectively shifted to θ and $\pi - \theta$.

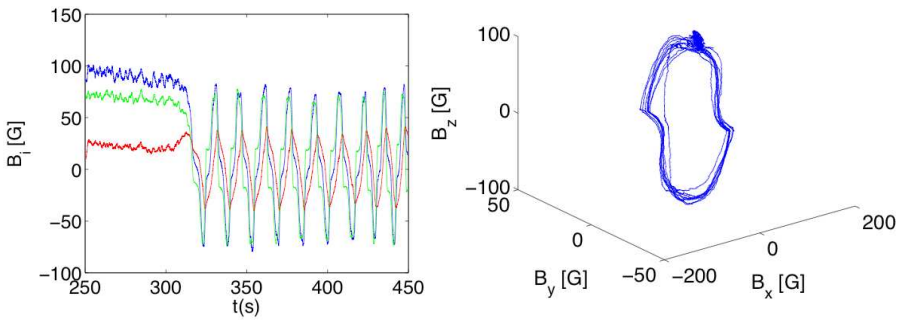

Figure 9: Transition from fixed point to a subcritical oscillatory dynamo. Left: time signal of the three components of the magnetic field. Right: Behavior in phase space.

When the torque is sufficiently strong, the stable and the unstable solutions collide and then bifurcate to a limit cycle. Near the relaxation oscillation, the dynamic of the field involves two different magnetic modes with close threshold: an axial dipole and a quadrupolar mode when propellers rotates at different frequencies. Experimentally we notice that a shift of the quadrupole along the rotation axis generates field reversals without variation of power.

The figure 10 shows a typical time signal of VKS experiment in the case of chaotic reversals. The dynamics seems very similar to the Earth and exhibits also some behavior called excursion, where the magnetic field temporarly decays but without reversing. Another interesting similarity with the Earth is the robustness of the reversals with respect to the turbulent fluctuations, especially the slow decay before a reversal followed by a fast recovery with a characteristic overshoot.

4.3 Model for VKS and geomagnetic reversals

This complicated behavior of the system can be well understood in the framework of a low-dimensional model, involving only the dipolar and quadrupolar modes [16]. The field can be decomposed as:

$$\mathbf{B} = d(t)\mathbf{D}(\mathbf{r}) + q(t)\mathbf{Q}(\mathbf{r}) \tag{6}$$

where $\mathbf{D}$ and $\mathbf{Q}$ represent the spatial structure of the dipolar and quadrupolar modes and $d(t)$ and $q(t)$ stand for the corresponding temporal evolution. In order to model the main feature of the magnetic field in a simple way, the study is restricted to the time evolution of the amplitudes d and q. The most general amplitude equations up to third order gives:

$$\dot{d} = \alpha_1 d + \beta_1 q + \gamma_{30} d^3 \gamma_{21} d^2 q + \gamma_{12} d q^2 + \gamma_{03} q^3 \tag{7}$$

$$\dot{q} = \alpha_2 q + \beta_2 d + \eta_{03} q^3 \eta_{21} d^2 q + \eta_{12} d q^2 + \eta_{30} d^3 \tag{8}$$

In exact counter-rotation, the problem presents a symmetry: a rotation of an angle π around a line in the equatorial plane. The two modes q and d can be classified into two different family depending on their behavior to this symmetry R_π. In the present case:

$$d \longrightarrow -d \tag{9}$$

$$q \longrightarrow q \tag{10}$$

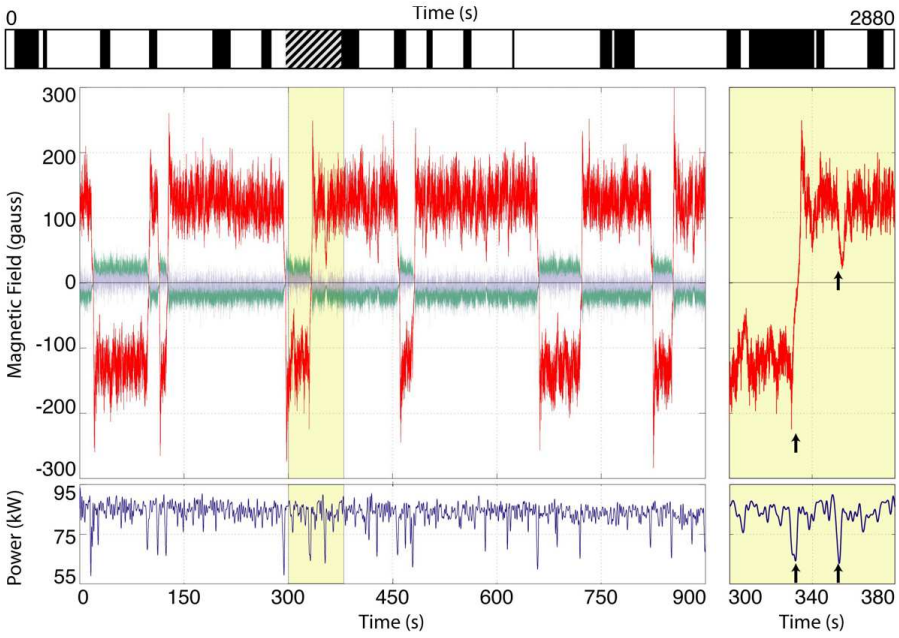

Figure 10: Time evolution of the magnetic field during reversal dynamics.

Under this symmetry, certain coefficients in equations 7 and 8 must vanish, giving

$$\dot{d} = \alpha_1 d + \gamma_{30} d^3 + \gamma_{12} d q^2 \quad (11)$$

$$\dot{q} = \alpha_2 q + \eta_{03} q^3 \eta_{21} d^2 q \quad (12)$$

Using the complex notation $A = d + iq = Re^{i\theta}$, we get the more compact form :

$$\dot{A} = \mu A + \nu \bar{A} + \lambda_1 A^3 + \lambda_2 A^2 \bar{A} + \lambda_3 A \bar{A}^2 + \lambda_4 \bar{A}^3 \quad (13)$$

where $\bar{A}$ is the complex conjugate of A. In the general case, the coefficients are complex and depend on the experimental parameters. The system can be understood by looking at the linear part of equation 13. The time evolution of the angle θ is given by the imaginary part of equation 13

$$\dot{\theta} = \mu_i - \nu_r \sin 2\theta \quad (14)$$

We remark that when $\mu = 0$, the equations respect the symmetry R_π and describe the experiment in exact counter-rotation regime. In this case, the equation for θ leads to 2 fixed points, $\theta = 0$ and $\theta = \pi/2$, corresponding respectively to the stable axial dipole and the damped quadrupole (figure 11a). In the non-exact counter-rotation, μ is increased and the symmetry R_π is broken. Therefore dipole and quadrupole can interact. The equations for the modes become:

$$\dot{d} = (\mu_r + \nu_r) d - \mu_i q \quad (15)$$

$$\dot{q} = (\mu_r - \nu_r) q + \mu_i d \quad (16)$$

The two modes bifurcate to instability at very close thresholds when ν is sufficiently small. Therefore μ_i represents the symmetry breaking and corresponds to the difference of rotation rate between the two discs for the VKS experiment. When this symmetry is broken, the unstable solution evolves away from the purely quadrupolar mode and evolves an increasing amount of dipolar component. The two modes (stable dipole and unstable quadrupole) become closer. When the system reaches $\mu_i = \nu_c$, a bifurcation occurs: each stable solution collides with an unstable solution and disappears. This a saddle node bifurcation that generates a limit cycle (thus an oscillatory magnetic field). This phenomenology is very similar to the one observed in the case of the pendulum with constant torque. However, a noteworthy difference occurs because of the additional symmetry $B \rightarrow -B$ yielding two other branches compared to the pendulum.

When $\mu_i \leq \nu_c$, the stable and unstable solutions are very close. When the system undergoes turbulent fluctuations, two different behavior can arise:

- When the fluctuation is larger than $\nu_c - \mu_i$, the system jumps from the stable to the unstable fixed points and then bifurcates to the $-B$ stable solution. The system had undergone a reversal associated with an overshoot (figure 11b).
- When the fluctuation is less than $\nu_c - \mu_i$, the system can deviate from the stable solution without reaching the unstable one and comes back on the stable solution. This is very similar to geomagnetic events called excursions (figure 11c).

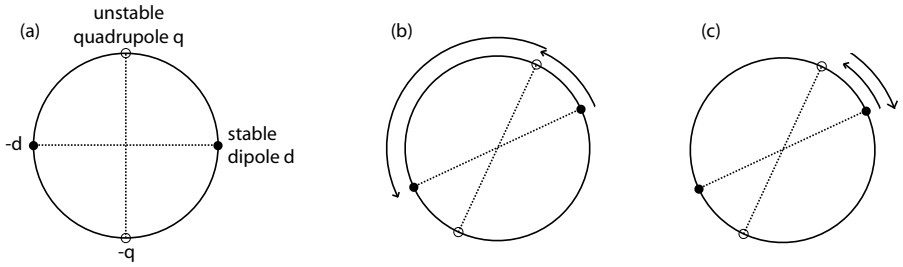

Figure 11: Three typical behaviors of the magnetic field. (a): Coexistence of two stationnary solution, stable and unstable when the symmetry R_π is respected. When R_π is broken, the interaction of dipolar and quadrupolar solutions can yields reversals (b) or simply excursions (c).

Using this simple model, the reversals of the VKS are understood as a consequence of the interaction of the axial dipole and the quadrupole. This interaction is related to the broken invariance of the flow under the rotation by π with respect to any axis in the mid-plane.

The magnetic field of the Earth also presents a competition between dipole and quadrupole. The symmetries involved in the case of the geodynamo are however different from the ones of the VKS experiment. In the core of the Earth, it is strongly believed that the flow is invariant under the mirror symmetry with respect to the equatorial plane. Under this

symmetry the dipole and the quadrupole can be classified into two different families. The previous model can thus naturally be applied to the case of the Earth. In this perspective, the reversals of the geomagnetic field could be caused by breaking the mirror symmetry of core dynamics.

5 Conclusion

- The VKS dynamo is not generated by the mean flow alone.
- The VKS experiment exhibits many different regimes in a small parameter range: stationary and oscillatory magnetic fields, reversals and excursions.
- A large scale dynamics of the field is observed: The results suggest that the system is governed by a few modes and this low dimensional dynamics is not smeared out by turbulent fluctuations.
- Using amplitude equation model, the reversals are understood to result from the competition between different modes (any external triggering mechanism are needed) and are due to a broken symmetry of the flow. A similar mechanism can be involved for planetary or stellar time dependent dynamos.

A Small and Large Re scaling of $\langle B^2 \rangle$

The flows creating the magnetic field of stars and galaxies involve huge kinetic, Re, and magnetic, Rm, Reynolds number. No laboratory experiments, nor direct numerical simulations are possible in the range of Re and Rm involved in astrophysical flows. It is thus interesting to try to guess scaling laws for the magnetic field using some simple hypotheses. This problem was first adressed by Batchelor for turbulent dynamos and is still an open question.

We consider here the minimum set of parameters: typical velocity V, length scale L, viscosity ν, magnetic permeability μ_0 and the fluid density ρ. We note that discarding global rotation makes our results certainly invalid for many astrophysical objects but not all of them. Rotation is indeed not assumed important for the galaxies which do not display a large scale coherent magnetic field [21],[20] and [4]. With 4 fundamental units, L (length), M (mass), T (time) and A (electric current), the problem involves 3 dimensionless parameters: $Rm = \mu_0 \sigma L V$, $Re = VL/\nu$ and $\langle B^2 \rangle / (\mu_0 \rho V^2)$. Some analytical calculations of threshold and saturation have been done for specific flow: for instance Childress and Soward for rotating $Rayleigh - Benard$ convection [6] or Busse with a more complicated case [5]. However, these kind of calculations are always very difficult because the problem is not self-adjoint.

A.1 Laminar scaling

The total velocity field V_0 can be decomposed as follow:

$$V_0 = V_c + V_1 \ , \tag{17}$$

where V_c is the flow at the dynamo threshold and V_1 is some additional flow depending on the distance from the onset. For the laminar regime, the Stokes force $\rho\nu\Delta V_1$ balances the Lorentz force $\mathbf{J}\times\mathbf{B}$ in the saturated regime and we can easily evaluate the amplitude:

$$\frac{\rho\nu V_1}{l^2} \sim \frac{B^2}{\mu_0 l} \ . \tag{18}$$

Using $Rm = \mu_0\sigma l V_0$ and $Rm_c = \mu_0\sigma l V_c$, we are left with the expression:

$$B^2 \sim \frac{\rho\nu}{\sigma l^2}(Rm - Rm_c) \ , \tag{19}$$

for the mean magnetic energy density in the non-linear saturated regime. This is a weak field regime and it is not really relevant for the Earth which is very far from a laminar regime.

A.2 Large Re scaling

When Re is very large, the Lorentz force is now balanced by the inertial term and we get:

$$\frac{B^2}{\mu_0 l} \sim \rho\frac{V_0 V_1}{l} \ . \tag{20}$$

Expressing this equation in term of magnetic Reynolds number yields:

$$B^2 \sim \frac{\rho}{\mu_0(\sigma l)^2}(Rm - Rm_c) \ . \tag{21}$$

One can note that the ratio between the two scalings 19 and 21 is the magnetic Prandtl number Pm.
In Geophysics, the well known strong field regime is supposed to appear in a subcritical bifurcation from the weak field branch. It is simple to show that taking into account the rotation leads to this strong field regime. By balancing the Coriolis force and the Lorentz force, the scaling becomes thus:

$$B^2 \sim \frac{\rho\Omega}{\sigma}(Rm - Rm_c) \ . \tag{22}$$

This scaling shows why most of the direct numerical simulations (DNS) of geodynamo find a good agreement with the satured value of magnetic field: all DNS generally manage to have the good ratio $\frac{\rho\Omega}{\sigma}$ despite Re or Ekman number being totally wrong.

B Turbulent Dynamos

As already stated, the problem of turbulent dynamos was proposed by Batchelor in 1950 [1]. In this paper, he looks at magnetic field generated by homogeneous isotropic turbulence with no mean helicity. Using a questionable analogy between the induction and the vorticity equations, he claimed that the dynamo threshold corresponds to $Pm = 1$, *i.e.* Rm_c proportional to Re, using our choice of dimensionless parameters. It is now often claimed

that Batchelor's criterion $Pm > 1$ for the growth of magnetic energy in turbulent flows is incorrect. It is however of interest to determine the minimal hypothesis for which Batchelor's predictions for dynamo onset is obtained using dimensional arguments. To wit, assume that the dynamo eigenmodes develop at small scales such that the threshold does not depend on the integral scale L. Then, discarding L in our set of parameters, dimensional analysis gives at once $Pm = Pm_c =$ constant for the dynamo threshold, *i.e.* Rm_c proportional to Re.

Another result of Batchelor concerns the saturation of the magnetic field. According to Batchelor's analogy between magnetic field and vorticity, the magnetic field should be generated mostly at the Kolmogorov scale, $l_K = LRe^{-3/4}$ where the velocity gradients are the strongest. He then assumed that saturation of the magnetic field takes place for $\langle B^2 \rangle / \mu_0$ proportional to $\rho v_K^2 K = \rho V^2 / \sqrt{Re}$ where v_K is the velocity increment at the Kolmogorov scale, $v_K^2 = \sqrt{\nu \epsilon}$. $\epsilon = V^3/L$ is the power per unit mass, cascading from L to l_K in the Kolmogorov description of turbulence. ϵ being the power per unit mass available to feed the dynamo, it may be a wise choice to keep it, instead of V in our set of parameters, thus becoming B, ρ, ϵ, L, ν, μ_0 and σ. Then, if we consider dynamo modes that do not depend on L, we obtain at once

$$\frac{B^2}{\mu_0} = \rho \sqrt{\nu \epsilon}\ h(Pm) = \frac{\rho V^2}{\sqrt{Re}}\ h(Pm)\ , \tag{23}$$

for saturation, where $h(Pm)$ is an arbitrary function of Pm. Close to dynamo threshold, $Pm \sim Pm_c$, we have $h(Pm) \propto Pm - Pm_c$ if the bifurcation is supercritical. This class of dynamos being small scale ones, it is not surprising that the inertial range of turbulence screens the magnetic field from the influence of integral size, thus L can be forgotten.

Some recent numerical simulations from Schekochihin [17] reported interesting behavior of the curve $Rm_c = f(Re)$. In these simulations of turbulent dynamo, one can observe that the threshold of the dynamo increases linearly with the Reynolds number on a large range of Re, according to Batchelor's theory. For sufficiently large Re, and using numerical hyperdiffusivity, the curve seems to saturate and to fall in the regime $Rm_c =$ constant.

Others results from Bierman and Schluter [3] show results compatible with the scenario of Scheckochihin for large Re. If Pm is small enough, the Kolmogorov and resistive scales are so far from each other that the magnetic field cannot feel the viscous dissipation. We can then drop ν in the analysis and we are left with $Rm_c =$ constant. In addition, discarding ν in the limit $Pm \ll 1$ gives:

$$\frac{B^2}{\mu_0} = \rho V^2 g_0(Rm)\ , \tag{24}$$

where g_0 is an arbitrary function. Close to threshold, the rms velocity V is given by $\mu_0 \sigma V L \sim Rm_c$. In the case of a supercritical bifurcation $g_0(Rm) \propto Rm - Rm_c$ and we obtain

$$B^2 \propto \frac{\rho}{\mu_0 (\sigma L)^2} (Rm - Rm_c)\ . \tag{25}$$

Far from threshold, $Re \gg Rm \gg Rm_c$, one could assume that B no longer depends on σ provided that the magnetic field mostly grows at scales larger than l_σ. We then obtain

equipartition between magnetic and kinetic energy densities

$$\frac{B^2}{\mu_0} \propto \rho V^2 \ , \tag{26}$$

as assumed by Biermann and Schluter.

C Evaluation of Ohmic dissipation

Ohmic losses due to currents generated by dynamo action give a lower bound to the power required to feed a dynamo. In order to evaluate them, it is crucial to know at which scales the magnetic field grows. Assuming that a dynamo is generated in the case $Pm \ll 1$, we want to give a possible guess for the power spectrum B^2 of the magnetic field as a function of the wave number k and the parameters ρ, ϵ, L, ν, μ_0 and σ. Far from threshold, $Re \gg Rm \gg Rm_c$, the dissipative lengths are such that $l_K \ll l_\sigma \ll L$. For k in the inertial range *i.e.* $kl_\sigma \ll 1 \ll kL$, we may use a Kolmogorov type argument and discard L, σ and ν. Then, only one dimensionless parameter is left and not too surprisingly, we get

$$|B|^2 \propto \mu_0 \rho \ \epsilon^{\frac{2}{3}} \ k^{-\frac{5}{3}} \ . \tag{27}$$

This is only one possibility among many others proposed for MHD turbulent spectra within the inertial range but it is the simplest. Integrating over k obviously gives the equipartition law for the magnetic energy. It is now interesting to evaluate Ohmic dissipation. Its dominant part comes from the current density at scale l_σ. We have

$$\frac{j^2}{\sigma} = \frac{1}{\sigma} \int |j|^2 dk \propto \frac{1}{\mu_0^2 \sigma} \int k^2 |B|^2 dk \propto \frac{\rho}{\mu_0 \sigma} \epsilon^{\frac{2}{3}} l_\sigma^{-\frac{4}{3}} \propto \rho \frac{V^3}{L} \ . \tag{28}$$

We thus find that Ohmic dissipation is proportional to the total available power which corresponds to some kind of optimum scaling law for Ohmic dissipation. Although, this does not give any indication that this regime is achieved, we note that the above scaling corresponds to the one found empirically from a set of numerical models. One can note that when the same derivation is applied for other scalings, different results are possible. For instance the k^{-1} spectrum yields a dissipation which can become greater than the input power. Thus the calculation of ohmic dissipation can invalidate the huge quantity of scaling present in the literature.

References

[1] G. K. Batchelor, *On the Spontaneous Magnetic Field in a Conducting Liquid in Turbulent Motion*, Royal Society of London Proceedings Series A, 201 (1950), pp. 405–416.

[2] Berhanu et al, *Magnetic field reversals in an experimental turbulent dynamo*, Europhys. Lett., 77 (2007), p. 59001.

[3] L. Biermann and A. Schlüter, *Cosmic Radiation and Cosmic Magnetic Fields. II. Origin of Cosmic Magnetic Fields*, Physical Review, 82 (1951), pp. 863–868.

[4] A. Brandenburg and K. Subramanian, *Astrophysical magnetic fields and nonlinear dynamo theory*, Phys. Rep., 417 (2005), pp. 1–4.

[5] F. H. Busse, *Nonlinear interaction of magnetic field and convection.*, Journal of Fluid Mechanics, 71 (1975), pp. 193–206.

[6] S. Childress and A. M. Soward, *Convection-Driven Hydromagnetic Dynamo*, Physical Review Letters, 29 (1972), pp. 837–839.

[7] Forest et al, Magnetohydrodynamics., 38 (2002), pp. 107–120.

[8] Gailitis et al, *Detection of a flow induced magnetic field eigenmode in the riga dynamo*, Phys. Rev. Lett., (2000).

[9] C. Gissinger, E. Dormy, and S. Fauve, *By-passing cowling's theorem in axisymmetric fluid dynamos*, arxiv, (2008).

[10] C. Gissinger, A. Iskakov, E. Dormy, and F. S., *Effect of magnetic boundary consitions on the dynamo threshold of von karman swirling flows*, Europhys. Lett., 82 (2008), p. 29001.

[11] G. Glatzmaier and P. H. Roberts, *A three-dimensional self-consistent computer simulation of a geomagnetic field reversal*, Nature, 377 (1995), pp. 203–209.

[12] H. Moffatt, *Magnetic field generation in electrically conducting fluids*, Cambridge University Press, (1978).

[13] Monchaux et al, *Generation of magnetic field by dynamo action in a turbulent flow of liquid sodium*, Phys. Rev. Lett., 98 (2007), p. 044502.

[14] Nataf et al, Geoph. Astroph. Fluids dyn., 100 (2006), pp. 281–298.

[15] F. Petrelis, N. Mordant, and S. Fauve, *On the magnetic fields generated by experimental dynamos*, G. A. F. D., 101 (2007), p. 289.

[16] Petrelis et al, *geomagnetic reversals caused by breaking mirror symmetry of core dynamics*, arxiv, (2008).

[17] A. A. Schekochihin, S. C. Cowley, S. F. Taylor, G. W. Hammett, J. L. Maron, and J. C. McWilliams, *Saturated State of the Nonlinear Small-Scale Dynamo*, Physical Review Letters, 92 (2004), pp. 084504–+.

[18] Sisan et al, Phys. Rev. Lett., 93 (2004), p. 114502.

[19] Stieglitz et al, *Experimental demonstration of a homogeneous two-scale dynamo*, Phys. of Fluids, 98 (2001), p. 044502.

[20] L. M. Widrow, *Origin of galactic and extragalactic magnetic fields*, Reviews of Modern Physics, 74 (2002), pp. 775–823.

[21] I. B. Zeldovich, A. A. Ruzmaikin, and D. D. Sokolov, eds., *Magnetic fields in astrophysics*, vol. 3, 1983.